S O N D E R D R U C K

aus

Proceedings of the
NORDERNEY SYMPOSIUM
on

SCIENTIFIC RESULTS OF THE GERMAN SPACELAB MISSION D1

Norderney, Germany, 27–29 August 1986

Editors

P.R. Sahm, RWTH Aachen, Germany
R. Jansen, BMFT Bonn, Germany
M.H. Keller, DFVLR Köln, Germany

Sponsored by:
German Ministry of Research and Technology (BMFT),
Bonn, Germany

THE ISOCHORIC SPECIFIC HEAT OF SULPHUR HEXAFLUORIDE SF_6 AT THE CRITICAL POINT UNDER μ-g CONDITIONS+

D1-MD-HPT 00

K. Nitsche and J. Straub
Lehrstuhl A für Thermodynamik
Technische Universität München, 8000 München, Germany

ABSTRACT

The specific heat a constant volume c_v shows a weak singularity at the critical point. Terrestrial measurements of c_v suffer from gravitational influences that increase drastically in the critical region due to the diverging compressibility. In order to investigate the critical behaviour of c_v in a homogeneous density field, the long-term experiment "Wärmekapazität" was performed during the D1-Mission in 1985. In the high precision thermostat HPT of the MEDEA double rack a four stage scanning ratio calorimeter was housed to continuously heat a fluid sample with 0.5 g SF_6 of critical density (ϱ_c = 0.737 g/cm^3) through the gas liquid critical point. Despite the reduced experiment time of four days, four different heating rates (dT/dt = 3.6, 10, 20 and 100 mK/h) could be accomplished. Data cover temperature spans around the critical point of /T-T_c/=50 and /T-T_c/=100 mK and were recorded with a density of 1 frame per 0.7 second.

Already a quasi-real-time data evaluation during the D1-Mission revealed one interesting result: The enhanced peak of c_v at the critical temperature (T_c=45.58°C) did not appear in any of the four runs, which contradicts literature predictions for μ-g environment. The critical "peak" appeared as a smooth hump instead of a sharp enhancement. 1g test runs after the mission evidenced proper hard ware performance of the calorimeter during the mission and correct cell filling for they showed the same critical enhancement as before the mission.

The data evaluation compares 1g and μg results for cell capacity C_0 and takes systematic errors into account. However, the results are still preliminary since the 1g measurements are not completed yet.

Key Words: Critical Phenomena, Critical Point, Isochoric Specific Heat, Scanning Ratio Calorimeter, Microgravity, Sulphur Hexfluoride, Material Properties.

1. INTRODUCTION

For a pure fluid the thermodynamic state of equilibirium is completely defined by two variables, e.g. temperature T and pressure p. Hence, the thermophysical properties derived from the equation of state are also functions of these two free variables. One important task in experimental thermodynamics is measuring material properties in order to establish empirical equations for real fluids. This common procedure requires time-consuming experimental work. Therefore, theoretical investigations aim at the computation of fluid properties solely as functions of the fluid's chemical composition and the free thermodynamic variables. Today's state of the art, however, does not yield such a general equation least for technical applications.

One notable exception is the vicinity of critical points. For the thermophysical behaviour of a system becomes independent of the physical microstructure. Singularities of fluid properties along certain paths through the critical region can be described using the same numerical values for the characteristic exponents and amplitude ratios regardless what substance is being investigated. The observed universality is not only confined to pure fluids it rather includes e.g. the critical decomposition of binary mixtures and solid body phenomena like the magnetisation at the Curie Point.

Highly accurate measurements in the critical region play an important role as references for establishing scaled equations of state [1,2]. As basic idea the scaled descriptions for the critical behavior incorporate that of critical universality. Systems belonging to the same universality class, characterized by the dimensions of space and the order parameter behave similarly. In this study the test fluid (SF_6), near its gas-liquid critical point, is classified by a scalar order parameter $\varrho_{gas} - \varrho_{liqu.}$ and behaves like a three-dimensional Ising system. For such a system macroscopic

+ Reprint from Proc. 6th European Symposium on Material Sciences under Microgravity Conditions, Bordeaux, ESA SP-256 (1987).

properties e.g. the specific heat c_v at constant volume can be theoretically derived. Especially renomalization group techniques have been applied which yield numerical values for critical expounds [3] and amplitude ratios [4,5], which are to be experimentally verified.

The gas-liquid critical point, however, seems to evade experimental access. The closer to it a refined thermometry and temperature control system allow accurate measurements, the more external fields distort the fluid's equilibrium. For example, in terrestrial experiments gravity falsifies specific heat measurements due to the diverging compressibility in the critical region. Even data from recent highly accurate experiments [6] especially designed for the asymptotic region exclude the immediate vicinity of the critical point.

This limitation for an experimental proof of the universality theory has led to the proposal a measure c_v along its critical isochore in a temperature window of $-100\ mK < (T-T_c) < +100\ mK$ under microgravity (µg) conditions, T_c being the critical temperature. These temperature bounds overlap regions for which reliable results, not affected by gravity, are available [6, 7, 8]. With the recorded µg behavior it was intended to fill the gap in the existing data set, in order to fit the asamptotic model

$$c_v = A\left|\frac{T-T_c}{T_c}\right|^{-\alpha} + B \qquad (1)$$

closer to the critical temperature.

The results in this work are assumed to be rather independent of gravitational fields, since the acceleration jitter showed an average level of less than $5\cdot10^{-5}$ g with occasional peaks during manouvering and sled runs. In order to quantify relaxational effects in the absence of gravity, now being of great influence upon phase transition, four temperature-time ramps (dT/dt=3.6, 10, 20 and 100 mK/h) could be accomplished within 4 days experimental time.

The sections below briefly outline the microgravity relevance of this experiment, scetch the principle of measurement and describe the considerations concerning the design of the test cell. The operational conditions are mentioned, how the experiment was governed from ground after it had fallen out of the official time-line. The documentation of the µg data display a comparison with related 1g measurements. However, the results are still to be considered as preliminary, since the data evaluation has not been completed yet. The discussion points out the discrepancy between µg and 1g data.

2. CRITICAL EXPONENTS AND MICROGRAVITY RELEVANCE

A quantification of critical anomalies is provided by power expressions describing state properties at the critical point. In the asymptotic region the shape of the background contribution is neglected and the equations are reduced to general exponental forms. The concept of universality, thereby, is physically based upon an increasing spacial extent of the fluctuations of the order parameter, which is of the same magnitude in different systems and represented by the correlation length

$$\xi = \xi_0\left|\frac{T-T_c}{T}\right|^{-\nu} . \qquad (2)$$

Of special theoretical interest is the specific heat c_v at constant colume, for it can be directly measured and describes the shape of the Helmholtz free energy function f:

$$c_v = -T\left(\frac{\partial^2 f}{\partial T^2}\right)_v . \qquad (3)$$

c_v shows a singularity in the critical region, as displayed in fig. 1 for water. Along the critical isochore within a limited temperature interval of about $/T-T_c/=50$ mK, c_v behaves according to Eq. (1).

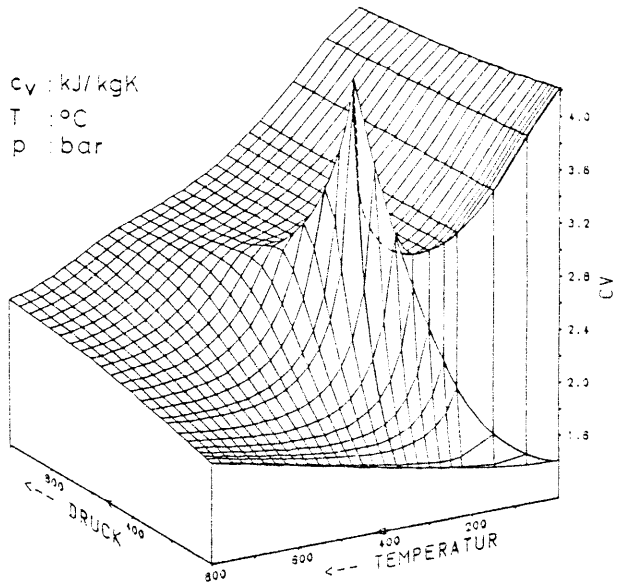

Fig. 1: The specific heat c_v of water versus temperature and pressure. c_v of the pure fluid SF_6 shows the same characteristical critical behavior, Schieber [19].

Caloric measurements require a minimum volume of test substance to be referred to. Much experimental effort is spent to suppress local gradients within the specimen. However, near the gas-liquid critical

point the diverging isothermal compressibility

$$K_T = \frac{1}{\rho}\left(\frac{\partial \rho}{\partial p}\right)_T \qquad (4)$$

leads to stratification of the density ϱ. For uniform temperature ($T < T_c$, $T=T_c$, $T > T_c$, Fig. 2) gravity distributes

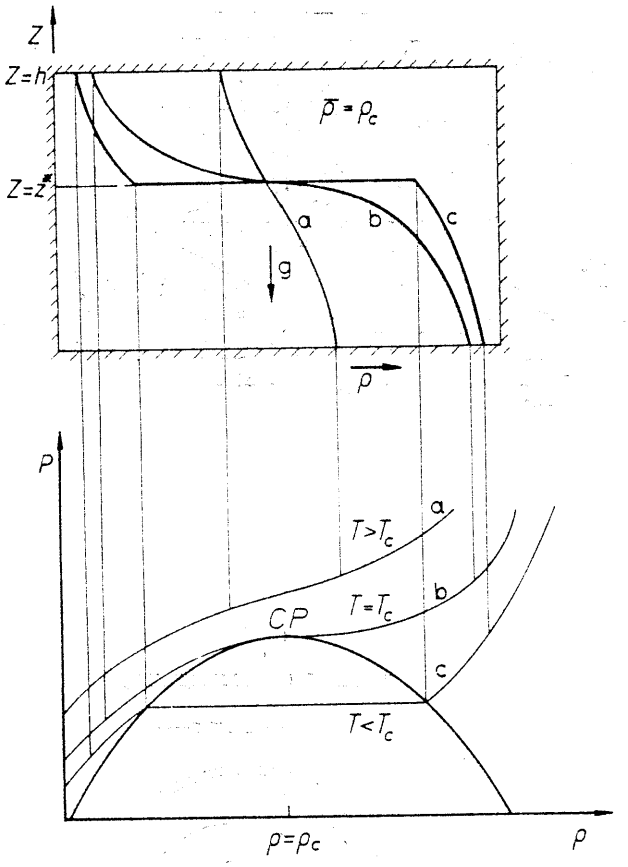

Fig. 2: Density stratification and the associated local states in a p-ϱ diagram of a pure fluid near its critical state under gravity. Temperature a: $T > T_c$, b: $T = T_c$, c: $T < T_c$. However the p-ϱ diagram does not show the correct pressure difference between the top and the bottom of the fluid container.

the density in the sample container of finite height h such that only a thin layer of thickness ξ at $z = z^*$ is of critical state ($T=T_c$, $\varrho = \varrho_c$ and $p=p_c$). Bulk measurements "somehow" integrate over all fluid states in the volume but are by no means average of local values. Thus, the c_v results represent a stretch of an isotherm rather than a point of state. In addition, while heating through the critical phase transition, gravity is considerably changing the density profile. Thus, an interpretation of c_v results has also to account for the systematic influence imposed by continuously rearranging the density field.

Measurements of the density as a function of the hydrostatic coordinate [9] agree

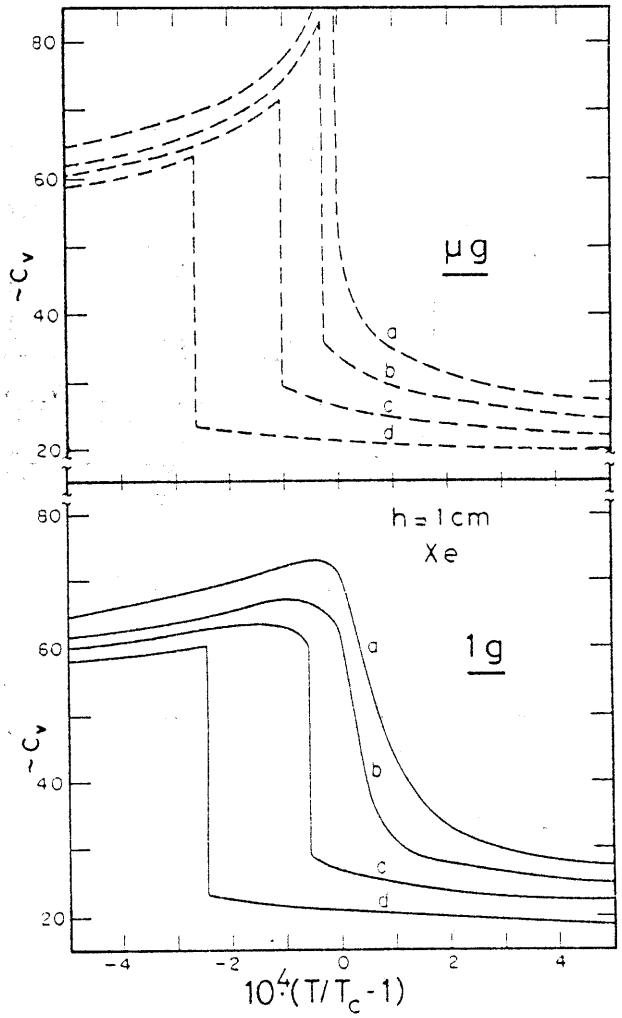

Fig. 3: Calculated specific heat of Xenon in dimensionless units under μg (upper part) and 1g conditions. Cell height: 1 cm, (ϱ/ϱ_c-1); a: 0, b: 0-044, c: 0.07, d: 0.10, Hohenberg and Barmatz [10].

with theoretical calculations. Numerical studies [10] modelling stratifications of ϱ yield the typical singular behaviour of c_v and extrapolate for μg conditions. Applying the linear model fig. 3 displays the characteristic of c_v versus reduced temperature for different reduced densities of the fluid Xenon. It is worthwhile to note that even for a deviation of 10% from the critical density, an apparent drop is theoretically predicted in a μg environment. Within the gravity affected temperature window $|\tau| = 3.5\cdot10^{-5}$ for CO_2 and $8\cdot10^{-5}$ for SF_6 ($\tau = T/T_c-1$)) the 1g curves are rounded and indicate that the maxima are somewhat shifted to below T_c. In earth-bound experiments the exact definition of T_c is determined either by data fitting, T_c being a free parameter, or by measuring the thermal relaxation times. Both values promise to coincide in space.

Finally, directly measuring the "true" form of the specific heat c_v under reduced gravity has been suggested in the respective

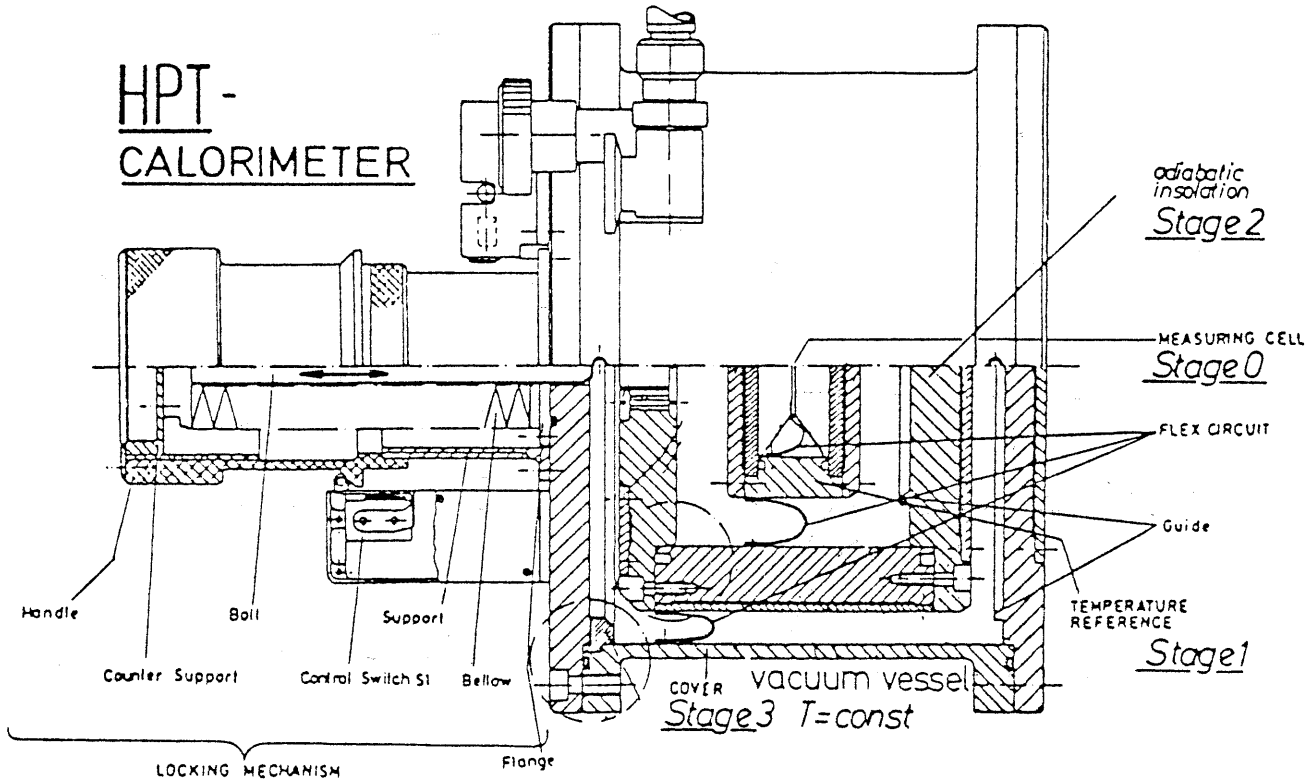

Fig. 4: Mechanical setup of the four stage HPT calorimeter.

literature [e.g. 11] in recent years as a consequent quest for verification of the theoretical models.

3. EXPERIMENTAL APPARATUS

The mechanical setup of the scanning ratio calorimeter used is shown in fig. 4. It resembles the one used by Lange [7] for c_v measurements and is described in greater detail in Ref. [12] together with the corresponding functional diagram. The mechanical structure consists of four cylindrical vessels (stage 0 - 3) boxed in each other. Specimen cell (0), stage 1 and 2 are heated through the critical temperature of SF_6 (45.583°C) on linear temperature-time ramps. The electronic control system minimizes temperature differences between the stages, thus shielding cell 0 adiabatically from external temperature fields.

The design of the coin-shaped test cell (Fig. 5) regards the following requirements: (i) a low heat capacity of the stainless steel shell (at T_c: C_{shell}/C_{fluid} = 1/1.2), (ii) sufficient mechanical resistance (p = 38 bar), (iii) a small hydrostatic height for terrestrial (1g) reference measurements. The inner spiral supporting the transverse faces divides the volume in a channel of 3*1 mm^2cross section wound around the center. Even near the critical state where the heat diffusivity goes to zero [13, 14] the heating power, input to stage 0, intrudes the test fluid

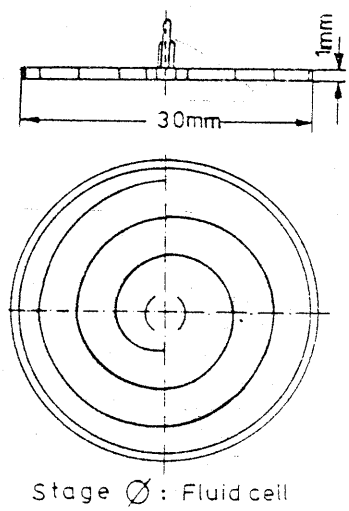

Fig. 5: Coin-shaped sample cell (stage 0).

equally distributed form the foil heater via numerous metal diffusion paths. Good thermal equilibrium in a metal shell is thereby accomplished.

4. MEASUREMENT METHOD

Applying an energy balance on stage 0 and 1 yields a system of differential equations

$$C_0 \cdot (dT_0/dt) = P_0 + P_{T,0} + \dot{Q}_{01} \qquad (5)$$

$$C_1 \cdot (dT_1/dt) = P_1 + P_{T,1} - \dot{Q}_{0,1} + \dot{Q}_{12} \qquad (6)$$

where $C_i.(dT_i/dt)$ denotes the capacity of stage i times the temperature ramp, P_i the electrical heating power, $\dot{Q}_{ij} - k_{ij}.(T_i T_j)$ the heat leakage from stage i to j, and $P_{T,i}$ the power dissipated in the thermistor i. P_i is measured applying four-wire techniques. To determine the interstage heat transfer $\dot{Q}_{ij}$, two methods are applicable:

(i) a stepwise increase of T_0-T_1 leads to a linear dependence of P_0, the heating power necessary to maintain the thermal inbalance in steady state, on the small temperature differences imposed. The coefficient k_{01} is the negative slope of a straight line P_0 versus T_0-T_1. This procedure, repeated for several process temperatures T_1-T_c, yielded constant slopes but a T_1-T_c dependent background term. This results from the divergence of the two thermistor characteristics in the servo loop for T_1-T_0, T^3 radiation effects being neglected. Thus, even for an output signal T_0-T_1=0, the calorimeter cell will lose or gain power to or from neighbouring stage 1 as a function of the overall process temperature T_1-T_c. Finally, a drift in the thermistors' resistance-temperature behaviour will ultimately change the background contribution but does not alter the caloric interstage coupling K_{ij}.

(ii) Five months had passed since the D1-Mission until the Spacelab HPT calorimeter was ready for 1g reference tests in the author's laboratory. Owing to this long period, subsequent readjustment of the AC-bridges is not very representative for an estimation of the thermal behaviour during the flight. The four different ramp rates dT/dt, however, permit a direct calibration of the interstage heat transfer as a function of T_1-T_c. An extrapolation to a temperature gradient dT/dt = 0 in equation (5) renders a simple relation $\dot{Q}_{01} = -P_{0,T} - P_{0,extrp}$, with $P_{0,extrp}$ extrapolated out of the values P_0 from four heating ramps at a certain process temperature T_1-T_c. $\dot{Q}_{01}$ calculated in such a manner can be linearly related to T_1-T_c.

Both ways (i and ii) to calibrate the calorimeter match with respect to the analysis of the 1g measurements and encourage to process the µg data as mentioned under (ii). Thus, knowing the coupling of the heating rate

$$dT_0dz = dT_1/dt + s\cdot(T_1 - T_c) \qquad (7)$$

governed by thermistor divergence, equation (7) combines (5) and (6) to an explicit function to the capacity C_0 from T_1-T_c, which can be further decomposed into

$$C_0(T_1-T_c) = C_{0,container} + m_{fluid}\cdot c_{v,fluid} \cdot \qquad (8)$$

$c_{v,fluid}$ denotes the specific heat of the test fluid to be measured versus temperature T_1-T_c.

5. QUASI-REAL-TIME DATA EVALUATION AND OFFNOMINAL EVENTS

Among the D1 fluid and material experiments, the HPT project to measure the specific heat showed a unique feature: The HPT CPU continuously output digital data and, thus, the final analysis did not have to be awaited to regognize the experiment's success or failure. These considerations brought about the transmitted data not only to be monitored during the mission, but also to be processed with respect to thermodynamic aspects. The authors installed their own HP-1000 laboratory computer with the complete periphery in the German ground station in Oberpfaffenhofen. Computer compatible tapes permitted transmission from the main mission data flux to the HP-1000 with a delay of 6 hours down to 2 hours in critical periods. Parallel to monitoring the calorimeter's house keeping (HK) values on CRT and xy-printer the complete mission performance of the HPT experiment was recorded on 144288 frames in a permanently updated data base with a time increment of 6 s. The decoding software demultiplexed

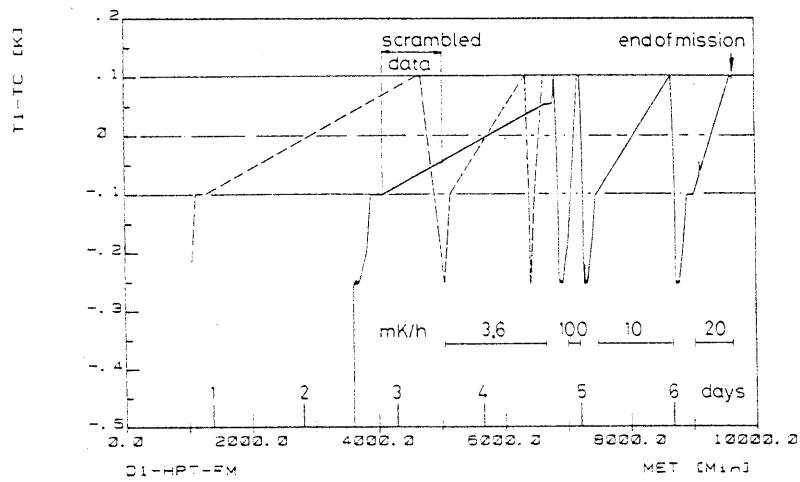

Fig. 6: Experimental time profile, dashed line: as planned, solid line as finally executed. MET: Mission ellapse time, the arrows indicate the period of scrambled data before the astronauts returned the lock-in amplifiers of the servo loop for T0-T1.

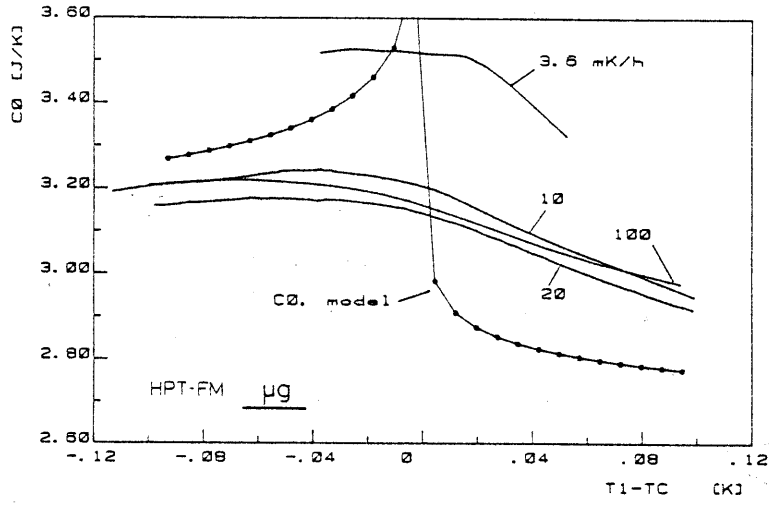

Fig. 7: Total cell capacity C_0, which is proportional to the specific heat c_v, under µg conditions versus the overall process temperature T_1-T_c. The curves represent four heating rates. The dotted line indicates the theoretical behaviour of C_0.

8.6 kBit/s and inserted real time and playback data, not always arriving in chronological order, into gaps of the data base.

The behavior of c_v, which was fragmentary at the moment due to gaps in the real-time coverage and which gradually became more complete after playback data had been inserted, was thus already available during the mission. In addition, xyz accelerometer plots indicated crew activities or a general jitter of less than 10-4 g. Both, quasi-real-time evaluation and HK monitoring helped to overcome hardware problems.

Fig. 6 documents the originally planned and finally executed experimental time profile as a plot of the overall process temperature T_1-T_c versus mission elapsed time MET. After an initial delay of two days (the ion getter pump of the calorimeter did not start owing to atmospheric pressure in the pre-evacuating vent line) one servo loop showed an anomal imbalance, which may have resulted from spontaneous thermistor drifting due to launch accelerations. This caused the heating power P_0, the measurement signal, to die out as T_1-T_c increased. An inevitable manuel readjustment of the lockin amplifier by the astronauts partly saved the first ramp and the accuracy of the complete experiment.

The subsequent ramps were not in tune with the official operational mission timeline. The initial problems finally changed into almost ideal experimental conditions. According to the plots of the data evaluation the investigators were able to adress their plans for the next run to the astronauts with an immediate response. Thus, the experiment was successfully completed at the end of the mission.

6. RESULTS

Data of the four gradients (3.6, 10, 20, 100 mK/h) were recorded with a density of 1264, 414, 180, 88 frames/mK during the mission and with 680, 579, 283, 85 frames/mK in the 1g runs. The further processing uses uniformly condensed data sets of 250 points for each ramp. Averaging reduces the noise to signal ratio and convents e.g. some 136137 frames raw data for the 3.6 mK/h ramp in toa manageabel amount of frames.

Fig. 7 and 8 display the results for the capacity C_0 under µg and 1g conditions,

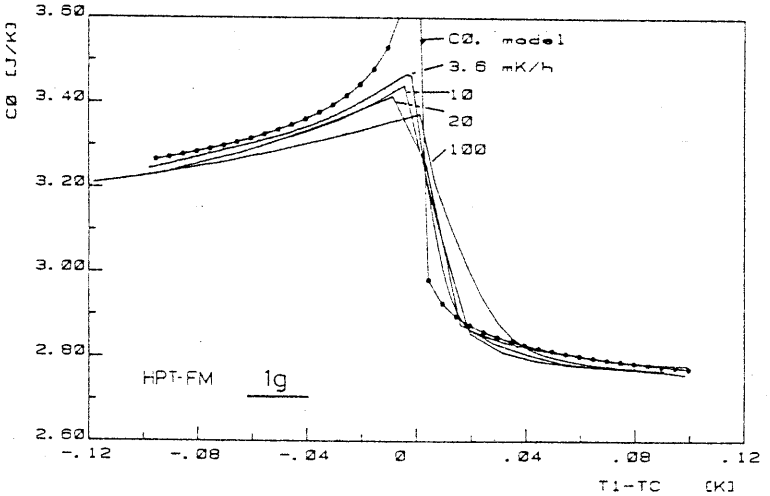

Fig. 8: Total cell capacity C_0 from 1g reference tests.

respectively, as a cubic spline representation. C_0 is proportional to the specific heat c_v according to equation 8. In addition to the curves for the four heating runs, a dotted line indicates the model behavior of equation (1), but recalculated for the complete cell capacity C_0. However, the computation contains an estimated value for the metal capacity of the cell shell. At least, it qualitatively reveals a theoretical guide line of how C_0 is "supposed" to be shaped. The maxima in the 1g lines may not be confused with the actual locations of the critical peaks relatively to each other, since gravity corrections ([10], [15]) have not yet been applied to the raw data.

7. DISCUSSION

At the current state of data evaluation the relative and absolute positions of the curves in fig. 7 and 8 are still preliminary. A refined analysis of the interstage heat transfer based upon more data points, as well as corrections of the process temperature T_1-T_c regarding non-linear bridge effects will cause a slight rotation and shift in the $C_0-(T_1-T_c)$ plane. Especially the profile for 3.6 mK ranges high and the one for 100 mK/h runs out of sequence. However, this will by no means explain the most obvious deviation of the µg curves from the 1g results: there is no evident peak in any of the µg runs.

C_0 reveals a surprisingly gentle rise and smooth drop and shapes rather a hump instead of an enhanced sharp peak as predicted (fig. 3). This unexpected behavior was confirmed in four sequential runs with different heating rates and gave rise to the suspicion the specimen cell may not contain SF_6 of critical density anymore. But even in this case a transition of first order would have exhibited a sudden drop as long density maintains a precision of $\pm$ 10 % of the critical value. Post mission g tests, however, evidenced correct filling and proper mission performance of the apparatus. This is also confirmed by comparing post and pre mission 1g data of the cell heating power P_0 which in both cases reveals no deviation from the characteristic critital behavior.

It is known that in earth-bound measurements, high ramp rates smear out a sharp transition peak for c_v as the coexistence curve is crossed. Depending on the ramp rate one can, in the immediate vicinity of the critical point, define or calculate [16] a window on the temperature scale within which data is rejected ($[\tau]$ $3\cdot10^{-5}$ for CO_2 and 3.6 mK/h [6], $[\tau] = 3.5\cdot10^{-5}$ for SF_6 and 3.6 mK/h [16]). Since the thermal diffusivity decreases towards the critical point, small temperature gradients imposed by the continuous heating method sustain in fluid volume. To account for this phenomenon quantified by the thermal relaxation time that on earth also shows a peak at the critical point, four different temperature ramps were run. A comparison of the 100 and 10 mK/h µg profiles shows even less a difference, although the ratio of the ramp rates is 10, than the cruves for 3.6 an 10 with a ratio of 2.7.

The conclusion is tempting that over the whole process temperature span the thermal equilibrium for each ramp rate is uniformly well maintained, since no significant change in the curvatures versus T_1-T_c emerges, that is confined to a limited region like in the 1g plots around the critical point. This is in accordance with earlier µg measurements [17] within the TEXUS program. The temperature in the center of a fluid sample of critical density followed, with an approximately constant delay, the leading temperature of the container, being linearly cooled and heated through the critical temperature. The demand for even lower heating rates, arising from the assumption that thermal equilibrium is even more retarded unter µg conditions, could not be realized. The calorimeter's noise to signal ratio would exceed a reasonable level and, moreover, the mission duration was limited. A ramp rate of 3.6 mK/h already corresponds to a rise in temperature of 1 degree in 11 days.

For further discussion the interphase boundary effects are considered. How does the shape of the meniscus affect phase transition? On earth, a flat meniscus spanning across the container perpendicular to the g-vector is a bottle neck for all interphase diffusion processes. The question whether an increased boundary can ease of hamper a c_v enhancement cannot be answered by simply tilting the calorimeter and, thus, reducing the meniscus area, since the ratio of critical state volume and total volume decreases as well from 0.1 percent to even less. This effect also smears out the peak of c_v.

In space a two pase fluid sample below T_c consists either of two macroscopically separated phase volumes, divided by an interface of measurable size and minimum surface energy or by a disperse emulsion of bubbles and droplets of almost infinite surface area. In both cases equilibrium is eased since the interface area is larger than that of the flat shape on earth. Therefore, thermal equilibrium is accelerated, since the "bottle neck" [18] of mass diffusion across the liquid vapour boundary is widened. A fine liquid vapour dispersion would, moreover, shorten the paths for mass diffusion compared to the rearrangement of 1g density profiles and, thus, cut down the associated relaxation time.

Let us add some final speculations for discussion: In case of thermal and mass diffusive equilibrium, a foamy liquid vapour system with its extended interface area

sets free an appreciable amount of surface energy while passing through the critical point. This may partly compensate for the external heating power necessary to increase the cell temperature linearly. The measured signals, heating current and voltage, associated with c_v, therefore, display no enhanced peak.

8. CONCLUSIONS

The German D1-Mission provided adequate conditions in microgravity environment for this experiment. With the help of the astronauts a contingency hardware malfunction could be overcome, that otherwise could have put the experiment into question. The apparatus was designed for manual adjustment. In four heating ramps the cell capacity C_0 was measured and showed reproducibly a smooth shape in the critical region instead of a sharp peak. The question whether relaxational effects are responsible for this unexpected behavior cannot be answered so far. Therefore, we suggest for future experiments at the critical point to additionally measure temperature at several locations directly in the fluid sample to record an established or distorted thermal equilibrium. Furthermore, optical techniques are necessary to learn about the density distribution of fluid at critical state under reduced weight. For both scientific objectives related proposis have been handed in to be realized in further µg-programs.

9. ACKNOWLEDGEMENTS

These investigations were sponsored by the German Bundesminister für Forschung and Technologie and were part of the D1-Mission program. The authors are also grateful to the German DFVLR for project management.

10. REFERENCE

[1] Griffiths, R.B.: Thermodynamic functions for fluids and ferromagnets near the critical point, Phys. Rev. 158, No.1 (1967).

[2] Widom, B.: The critical point and scaling theorey, Phsica 73, 107 (1974).

[3] Baker, G.A., Nickel, Jr., Meiron, P.I.: Critical indices from perturbation analysis of the Callan-Symanzik equation, Phys. Rev. B17, 1365 (1976).

[4] Bervillier, C.: Universal relations among critical amplitudes. Calculations up to order epsilon^2 for systems with continuous symmetry, Phys. Rev. B14, 4964 (1976).

[5] Brézin, E., Le Guillou, J.G., Zinn-Justin, J.: Approach to scaling in renormalized pertubation theory, Phys. Rev. D8, 2418 (1973).

[6] Edwards, T.J.: Specific heat measurements near the critical point of carbon dioxide, thesis, Department of Physic, University of Western Australia (1984).

[7] Lange, R., Straub, J.: Die isochore Wärmekapazität fluider Stoffe im kritischen Gebiet - Voruntersuchungen zu einem Spacelab-Experiment, BMFTFB-W 84-034 (1984).

[8] Straub, J., Lange, R., Nitsche, K., Kemmerle, K.: Isochoric specific heat of sulfur hexafluoride at the critical Point. Laboratory results and outline of a Spacelab experiment for the D1-Mission in 1985, Int.J.of Thermophysics, Vol. 7, No. 2, 343 (1986).

[9] Straub, J.: Kritische Phänomene in Fluiden, Habilitationsschrift, Technische Universität München (1977).

[10] Hohenberg, P.C., Barmatz, M.: Gravity effects near the gas-liquid critical point, Phys. Rev. A6, No.1, 289 (1972).

[11] Sengers, J.V., Moldover, M.R.: Critical Phenomena Experiments in Space?, Z. Flugwiss. u.Weltraumfor. 2, Heft 6 (1978).

[12] Nitsche, K., Straub, J., Lange, R.: Isochoric specific heat of sulfur hexafluoride at the critical point - a Spacelab experiment for the German D1-Mission in 1985, Proceed. 5 th European Symposium on Material Sciences under Microgravity -Schloss Elmau, ESA SP 222, 335 (1985).

[13] Reile, E., Jany, P., Straub, J.: Messung der Temperaturleitfähigkeit reiner Fluide und binärer Gemische mit Hilfe der dynamischen Lichtstreuung, Wärme- und Stoffübertragung 18, 99 (1984).

[14] Swinney, H.L., Cummins, H.Z.: Thermal diffusivity of carbon dioxide in the critical region, Phys. Rev. 171, No. 1, 152 (1968).

[15] Lipa, J.A., Edwards, C., Buckingham, M.J.: Specific heat of CO_2 near the critical point, Phys. Rev. A, 15, 778 (1977).

[16] Lange, R.: Die Anomalie der isochoren Wärmekapazität im kritischen Gebiet von Schwefelhexafluorid, Dissertation, Technische Universität München (1983).

[17] Nitsche, K., Straub, J., Lange, R.: Ergeonisse des TEXUS-8-Experiments 'Phasenumwandlung', Forschungsbericht Luft- und Raumfahrt, BMFT (1984).

[18] Dahl, D., Moldover, M.R.: Thermal relaxation near the critical point", Phys. Rev.A, Vol.6, No.5, 1915 (1972).

[19] Schiebener, P., at Lehrstuhl A für Thermodynamik, TU München, Arcisstr. 21, 8000 München 2, FRG.